



Journal of Applied and Computational Mechanics



Research Paper

A Novel Exponential Zigzag Function Coupled High-order Beam Theory for Advanced Laminated Composite Analysis

Leonardo Fellipe Prado Leite^{ID}, Fabio Carlos da Rocha^{ID}

Department of Civil Engineering, Laboratory of Building Materials and Structures (LAMCE), Federal University of Sergipe, São Cristóvão, Aracaju-SE, 49100-000, Brazil
Email: leolvp@academico.ufs.br (L.F.P.L.); fabiocrocha@academico.ufs.br (F.C.R.)

Received October 01 2023; Revised December 10 2023; Accepted for publication December 10 2023.

Corresponding author: F.C. da Rocha (fabiocrocha@academico.ufs.br)

© 2023 Published by Shahid Chamran University of Ahvaz

Abstract. Various industrial sectors require highly specialized and efficient materials for applications in fields such as the military, aeronautics, aerospace, and mechanical and civil engineering. Composite materials that meet the stringent requirements across these domains have become prominent, often serving as structural components and requiring precise mathematical modeling. Zigzag (ZZ) and Layerwise (LW) theories are commonly used for laminated-beam structural analysis. Although the LW theory provides superior accuracy, it suffers from an increase in unknowns as the number of layers grows. Conversely, the ZZ theory is less computationally intensive and less accurate. This study proposes an exponential high-order zigzag function with a unified kinematic formulation to enhance the accuracy of the ZZ theory. The results were compared with those of existing models and demonstrated excellent agreement with the reference solutions, irrespective of the layer count or slenderness index, making it a more efficient choice for laminated-beam analysis.

Keywords Laminated Composite Beams, High Order Beam Theory, Zigzag Theory, High-Order Zigzag function, Layerwise Theory.

1. Introduction

Several formulations have been developed to describe the structural behavior of beams. The best-known and most straightforward theory is the classical Euler-Bernoulli (TEB) [1]. However, the TEB is suitable for modeling beams with a small height-to-length ratio because it does not consider shear strain. To overcome this limitation, a first-order theory for shear strain, also known as the Timoshenko beam theory (TBT), was developed [2]. Although the TBT incorporates the shear effect, it has some notable shortcomings. These include nonzero shear stresses at the upper and lower edges of the beam, the absence of the cross-sectional warping effect, inadequate representation of the shear stress field distribution in the cross-section, and the need to use correction factors [2].

Higher-order kinematics, also known as high-order theories for beams, have been developed to overcome the difficulties associated with Timoshenko's theory. Among the relevant proposals in this context, those by Krusweski [3], Reddy [4], Touratier [5], Soldatos [6], Karama [7], and Akavci [8] stand out. Such advanced approaches aim to improve the description of the structural behavior of beams, covering aspects that need to be duly considered by the TEB and TBT, such as a more accurate distribution of shear stresses and consideration of cross-section warping. Generally, high-order kinematics is used to analyze beams made of a single material. However, composite materials provide greater possibilities for the composition of materials and for obtaining the desired properties efficiently. These materials require more accurate mechanical analysis, which makes the application of higher-order kinematics attractive.

To analyze laminated composite beams more accurately, new parameters must be incorporated into the kinematics to capture the interactions between laminations and their individual behaviors [9]. The equivalent single-layer (ESL), layerwise (LW), and zigzag (ZZ) theories are examples of the main formulations used in this analysis [10].

The LW and ZZ theories separately address the behavior of each lamina, providing superior accuracy over the ESL theory. However, the LW theory has a disadvantage in terms of computational cost because the number of unknowns increases proportionally with the number of layers. The ZZ approach was developed to make the number of unknowns independent of the number of layers without significantly compromising the accuracy of the results. This approach incorporates the zigzag effect into ESL theories [10]. This approach offers a viable solution that balances the computational efficiency and accuracy of laminated composite beam analyses.

Owing to the independence between the number of layers and the unknown parameters of the problem, several studies related to the zigzag theory have been conducted. Murakami [11] developed a function called "zigzag," which incorporates only geometric information, and applied it to TBT. Similarly, Di Sciuva [12] formulated a zigzag theory using the Heaviside function. In 1987 [13], a cubic term was added to the kinematics to analyze plate problems. To overcome the challenges in determining the stress fields for the Timoshenko beam theory (TBT), Di Sciuva and Gherlone [14] developed a refined zigzag theory (RZT) that



circumvents the difficulties in determining these fields. Lurlaro [15] compared the RZT with other beam theories and evaluated their buckling and bending behaviors. In this study, the differences between the stress fields calculated using equilibrium equations and those computed using constitutive relations were observed.

Vidal [16] combined Murakami's zigzag function with high-order kinematics in a sinusoidal format, resulting in greater precision in the displacement and stress fields. Similarly, Zhen [17] obtained better results by combining the sinusoidal kinematics proposed in [4] with a high-order zigzag function in a polynomial format. Leite and Rocha [18] proposed a new zigzag function combined with a unified formulation that incorporates several higher-order theories. Leite and Rocha [18] concluded that combining the ZZ and kinematic functions, both of high order, provides accurate results. However, in [18], the authors suggested that the combination of their proposed function and the high-order kinematics proposed by Soldatos [6] presented better results than the other kinematics studied in their work.

Previous works [16-18] show that better results were obtained for mechanical response fields of interest when refined beam theories were combined with high-order zigzag functions. Therefore, the present work proposes a novel high-order zigzag function coupled with a unified formulation for high-order beam theory. The present proposal aims to increase the accuracy of the results compared to other zigzag functions already considered in the literature. Existing zigzag theories present difficulties in accurately obtaining the response fields, especially for shear stress. Therefore, the present proposal is an alternative for overcoming this deficiency without increasing the number of unknowns as the number of layers in the laminate increases. Based on this proposed model, a comparative analysis is carried out, aiming to evaluate the accuracy between different refined approaches to beams when associated with the exponential ZZ function, as well as other ZZ functions present in the literature and/or together with the LW theory, when there are results available in the literature for the latter. The structure of this work is as follows: In Section 2, the necessary domain and boundary restrictions are established to ensure that the first variation of the total energy functional is equal to zero. Section 3 presents the Navier procedure to determine a solution to the problem proposed in the previous section. Section 4 presents and discusses the results. Finally, the conclusions drawn from this study are presented in Section 5.

2. Mathematical Development

2.1 Definitions

Consider a composite beam with a total thickness and length of $2h$ and $L = x_b - x_a$, respectively, subjected to a distributed load $q(x)$, traction (external forces per unit area) $T_{x\alpha}$, and $T_{z\alpha}$ with $(\alpha = a, b)$, as shown in Fig. 1. In the cross section, the thickness of each layer was identified by $2h^{(k)}$, with $k = 1, 2, \dots, N$ representing the layer numbering. The ordinates of the interfaces between each layer are provided by $z_{(i)} (i = 0, 1, \dots, N)$, $z_0 = -h$, $z_N = h$, and $z_{(k)} = z_{(k-1)} + 2h^{(k)}$, as shown in Fig. 2.

2.2 Kinematics

The present formulation considers the linear elastic behavior of the material. The displacement fields of various beam theories considering shear strain were chosen and unified based on the following hypotheses:

- (1) There is no deformation in the transverse direction.
- (2) The bending component of the axial displacement is similar to that of the classical beam theory.
- (3) The shear component of the axial displacement provided high-order variations in the stress and strain such that these response fields were zero on the upper and lower surfaces.
- (4) Axial displacement in a zigzag form was achieved by inserting a new function into the laminated composite.

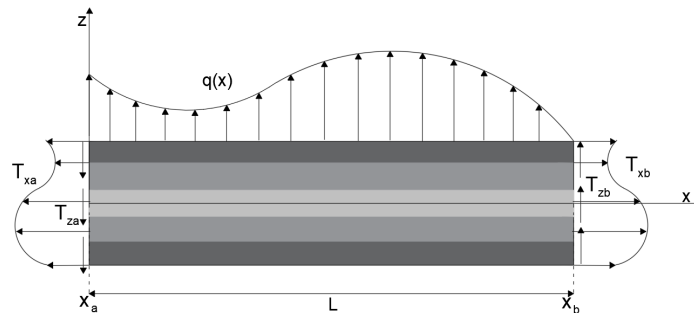


Fig. 1. Laminated composite beam subjected to external loads.

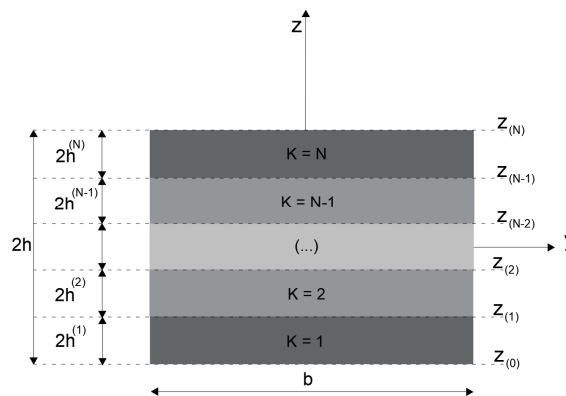


Fig. 2. Geometric information of the cross section in the laminated beam.



Table 1. Shear distribution function for higher order kinematics.

Author	$f(z)$
Kruszewski (1949) [3] - KRU49	$\frac{5z}{4} \left(1 - \frac{4z^2}{12h^2} \right)$
Reddy (1990) [4] - RED90	$z \left(1 - \frac{4z^2}{12h^2} \right)$
Tourratier (1991) [5] - TOU91	$\frac{5h}{\pi} \sin \left(\frac{\pi z}{2h} \right)$
Soldatos (1992) [6] - SOL92	$z \cosh \left(\frac{z}{2} \right) - 2h \sinh \left(\frac{z}{2h} \right)$
Karama (2003) [7] - KAR03	$z \exp \left[-2 \left(\frac{z}{2h} \right)^2 \right]$
Akavci (2007) [8] - AKA07	$\left(\frac{3\pi}{2} \right) \left[2h \tanh \left(\frac{z}{2h} \right) - z \sec^2 h \left(\frac{1}{2} \right) \right]$

Based on these assumptions, the displacement fields for various beam theories with high-order shear strain and zigzag functions are expressed by:

$$\begin{aligned} u^{(k)}(x, z) &= u_0(x) - zw_0'(x) + f(z)\Phi(x) + \Phi_{zz}^{(k)}(z)\psi(x), \\ w(x, z) &= w_0(x), \end{aligned} \tag{1}$$

where $w(x)$ and $u^{(k)}(x, z)$ are the transverse (z -axis) and axial displacements (x -axis) of each layer, respectively; $w_0(x)$ and $u_0(x)$ are the transverse and axial displacements in the middle plane of the beam, respectively; $f(z)$ is a function that represents the distribution of high-order shear stress and strain along the depth of the beam (Table 1); $\Phi(x)$ is the angle due to shear; $\Phi_{zz}^{(k)}(z)$ is a function that provides the “zigzag behavior”; and $\psi(x)$ is a zigzag amplitude function. The apostrophes above these functions represent the derivatives of the variable function.

From Eq. (1), the linear elastic strain field can be expressed as follows:

$$\begin{aligned} \varepsilon^{(k)}(x, z) &= \frac{\partial u^{(k)}(x, z)}{\partial x} = u_0'(x) - z w_0''(x) + f(z)\Phi'(x) + \Phi_{zz}^{(k)}(z)\psi'(x), \\ \gamma^{(k)}(x, z) &= \frac{\partial w(x)}{\partial x} + \frac{\partial u^{(k)}(x, z)}{\partial z} = f'(z)\Phi(x) + \beta(z)\psi(x), \end{aligned} \tag{2}$$

such that $\beta(z)$ is the first derivative of the “zigzag” function concerning z . The shear and normal stresses of fibrous orthotropic materials can also be expressed using the constitutive equation presented as follows:

$$\begin{aligned} \sigma^{(k)}(x, z) &= \overline{Q_{11}^{(k)}} \varepsilon^{(k)}(x, z) = \overline{Q_{11}^{(k)}} [u_0'(x) - z w_0''(x) + f(z)\Phi'(x) + \Phi_{zz}^{(k)}(z)\psi'(x)], \\ \tau^{(k)}(x, z) &= \overline{Q_{55}^{(k)}} \gamma^{(k)}(x, z) = \overline{Q_{55}^{(k)}} [f'(z)\Phi(x) + \beta(z)\psi(x)], \end{aligned} \tag{3}$$

where $\overline{Q_{11}^{(k)}}$ and $\overline{Q_{55}^{(k)}}$ are the reduced elastic properties of fiber-reinforced orthotropic materials in the plane strain state [11].

A new format for the zigzag function, $\Phi_{zz}(z)$, with exponential behavior, called ZZ-EXP, as described in Eq. (4), is proposed in this study. This proposal incorporates Murakami’s [11] zigzag linear function (see Eq. (5)) and satisfies the following conditions:

- (1) “zigzag” behavior to beam axial displacement fields.
- (2) Nullity of shear stresses on the upper and lower edges of the laminate, that is, $\tau(1)(x, z(0)) = \tau(N)(x, z(N)) = 0$.

$$\Phi_{ZZ}^{(k)}(z) = e^{(2h^{(k)})^3 [\Phi_{ZZ-MUR}^{(k)}(z)]} - \left[\frac{z^2}{2z_0} + \left(\frac{2z^3 - 3z_0 z^2}{12z_N^2} \right) \right] e^{(2h^{(k)})} \frac{d\Phi_{ZZ-MUR}^{(0)}(z)}{dz} - \left(\frac{2z^3 - 3z_0 z^2}{12z_N^2} \right) e^{(2h^{(k)})} \frac{d\Phi_{ZZ-MUR}^{(N)}(z)}{dz} \tag{4}$$

$$\Phi_{ZZ-MUR}^{(k)}(z) = (-1^{(k)}) \frac{[-2z + (z^{(k)} + z^{(k-1)})]}{2h^{(k)}} \tag{5}$$

In Fig. 3, the behaviors of the proposed and Murakami’s [11] functions are compared for a three-layer laminate. ZZ-EXP displays a curved distribution in the outer layers, which is notably different from the behavior proposed in [11].

2.3 Governing equations

Virtual work principle (VWP) is used to develop the governing equations, and the following equation represents their general expression:

$$\delta W_{int} - \delta W_{ext} = 0. \tag{6}$$

where δW_{int} is the internal work expressed in Eq. (7), and δW_{ext} is the external work expressed in Eq. (8) according to the loading shown in Fig. 1.

$$\delta W_{int} = \int_V (\sigma^{(k)}(x, z)\delta\varepsilon^{(k)}(x, z) + \tau^{(k)}(x, z)\delta\gamma^{(k)}(x, z)) dV. \tag{7}$$

$$\delta W_{Ext} = \int_{x_a}^{x_b} q(x)\delta w_0(x)dx + \int_A [T_{x_a} \delta u^{(k)}(x_a, z) + T_{z_a} \delta w_0(x_a)] dA - \int_A [T_{x_b} \delta u^{(k)}(x_b, z) + T_{z_b} \delta w_0(x_b)] dA. \tag{8}$$



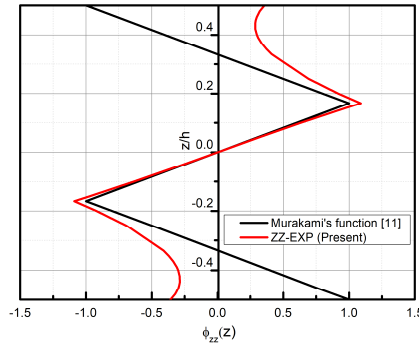


Fig. 3. Zigzag functions are linear [11] and exponential (present) for a regular laminate with three layers.

Such that $T_{x\Delta} = T_x(x_\Delta, z)$, $T_{z\Delta} = T_z(x_\Delta, z)$ are tractions (with $\Delta = a$ or $\Delta = b$), and $q(x)$ is the load on the structure. Eqs. (1)–(3) are substituted in Eqs. (6)–(8), and Euler's Equation is obtained using the fundamental lemma of variational calculus. The restrictions imposed to obtain the Euler equation led to the differential equilibrium equations and their boundary conditions, respectively, in Eqs. (9) and (10).

$$\begin{aligned} \frac{\partial N_x(x, z)}{\partial x} &= 0, & \frac{\partial^2 M_x(x, z)}{\partial x^2} &= q(x), \\ \frac{\partial M_\phi(x, z)}{\partial x} &= V_\phi(x, z), & \frac{\partial M_{zz}(x, z)}{\partial x} &= V_\beta(x, z). \end{aligned} \tag{9}$$

$$\begin{aligned} N_x(x_\Delta, z) &= \bar{N}_x(x_\Delta, z) \text{ or } u_0(x_\Delta) = \bar{u}_0(x_\Delta), & M_x(x_\Delta, z) &= \bar{M}_x(x_\Delta, z) \text{ or } w'(x_\Delta) = \bar{w}'(x_\Delta), \\ M_\phi(x_\Delta, z) &= \bar{M}_\phi(x_\Delta, z) \text{ or } \Phi(x_\Delta) = \bar{\Phi}(x_\Delta), & M_{zz}(x_\Delta, z) &= \bar{M}_{zz}(x_\Delta, z) \text{ or } \psi(x_\Delta) = \bar{\psi}(x_\Delta), \\ V_x(x_\Delta, z) &= \bar{V}_x(x_\Delta, z) \text{ or } w(x_\Delta) = \bar{w}(x_\Delta), & & \text{with } \Delta = a \text{ or } b. \end{aligned} \tag{10}$$

$$\begin{aligned} N_x(x, z) &= \int_A \sigma^{(k)}(x, z) dA & M_x(x, z) &= \int_A z \sigma^{(k)}(x, z) dA & M_\phi(x, z) &= \int_A f(z) \sigma^{(k)}(x, z) dA \\ M_{zz}(x, z) &= \int_A \Phi_{zz}^{(k)}(z) \sigma^{(k)}(x, z) dA & V_\phi(x, z) &= \int_A f'(z) \tau^{(k)}(x, z) dA & V_\beta(x, z) &= \int_A \beta^{(k)}(z) \tau^{(k)}(x, z) dA \end{aligned}$$

Rewriting Eq. (9) in terms of the displacements, rotations, and amplitudes of the ZZ function, the following equation was obtained:

$$\begin{aligned} Au_0''(x) - A_z w''''(x) + B\Phi''(x) + D\psi''(x) &= 0, \\ A_z u_0''''(x) - A_{zz} w''''(x) + B_z \Phi''''(x) + D_z \psi''''(x) &= q(x), \\ Bu_0''(x) - B_z w''''(x) + B_f \Phi''(x) + D_f \psi''(x) &= G_f \Phi(x) + G_\psi \psi(x), \\ Du_0''(x) - D_z w''''(x) + D_f \Phi''(x) + D_\phi \psi''(x) &= G\Phi(x) + G_\beta \psi(x). \end{aligned} \tag{11}$$

where,

$$\begin{aligned} \begin{bmatrix} A \\ A_z \\ A_{zz} \end{bmatrix} &= b \sum_{k=1}^N \int_{z^{(k-1)}}^{z^{(k)}} \begin{bmatrix} \bar{Q}_{11}^{(k)} \\ z \bar{Q}_{11}^{(k)} \\ z^2 \bar{Q}_{11}^{(k)} \end{bmatrix} dz, & \begin{bmatrix} B \\ B_z \\ B_f \end{bmatrix} &= b \sum_{k=1}^N \int_{z^{(k-1)}}^{z^{(k)}} \begin{bmatrix} f(z) \bar{Q}_{11}^{(k)} \\ z f(z) \bar{Q}_{11}^{(k)} \\ f(z)^2 \bar{Q}_{11}^{(k)} \end{bmatrix} dz, & \begin{bmatrix} \bar{N}_x(x_\Delta, z) \\ \bar{M}_x(x_\Delta, z) \\ \bar{M}_\phi(x_\Delta, z) \\ \bar{M}_{zz}(x_\Delta, z) \\ \bar{V}_x(x_\Delta, z) \end{bmatrix} &= b \sum_{k=1}^N \int_{z^{(k-1)}}^{z^{(k)}} \begin{bmatrix} T_{x\Delta} \\ z T_{x\Delta} \\ f(z) T_{x\Delta} \\ \Phi_{zz}^{(k)}(z) T_{x\Delta} \\ T_{z\Delta}(z) \end{bmatrix} dz \\ \begin{bmatrix} D \\ D_z \\ D_f \\ D_\phi \end{bmatrix} &= b \sum_{k=1}^N \int_{z^{(k-1)}}^{z^{(k)}} \begin{bmatrix} \Phi_{zz}^{(k)}(z) \bar{Q}_{11}^{(k)} \\ z \Phi_{zz}^{(k)}(z) \bar{Q}_{11}^{(k)} \\ f(z) \Phi_{zz}^{(k)}(z) \bar{Q}_{11}^{(k)} \\ \Phi_{zz}^{(k)2}(z) \bar{Q}_{11}^{(k)} \end{bmatrix} dz, & \begin{bmatrix} G \\ G_f \\ G_\beta \end{bmatrix} &= b \sum_{k=1}^N \int_{z^{(k-1)}}^{z^{(k)}} \begin{bmatrix} f'(z) \beta^{(k)}(z) \bar{Q}_{55}^{(k)} \\ f'(z)^2 \bar{Q}_{55}^{(k)} \\ \beta^{(k)}(z)^2 \bar{Q}_{55}^{(k)} \end{bmatrix} dz \end{aligned} \tag{12}$$

2.4 Analytical solution

The Navier procedure was used to solve the differential equations for equilibrium (Eq. (11)). In this procedure, response fields are approximated using periodic functions with separate variables. The boundary conditions for a simply supported beam are given by Eq. (13), and the solution is assumed to conform to Eq. (14):

$$\begin{aligned} w(0) &= M_x(0, z) = M_\phi(0, z) = M_{zz}(0, z) = 0 \\ w(L) &= M_x(L, z) = M_\phi(L, z) = M_{zz}(L, z) = 0 \end{aligned} \tag{13}$$

$$\begin{aligned} w(x) &= \sum_{j=1}^\infty w_j \sin\left(\frac{j\pi x}{L}\right), & u_0(x) &= \sum_{j=1}^\infty u_{0j} \cos\left(\frac{j\pi x}{L}\right) \\ \Phi(x) &= \sum_{j=1}^\infty \Phi_j \cos\left(\frac{j\pi x}{L}\right), & \psi(x) &= \sum_{j=1}^\infty \psi_j \cos\left(\frac{j\pi x}{L}\right) \end{aligned} \tag{14}$$



Table 2. Maximum values and relative errors considering the results of Pagano [19] as reference.

$f(z)$	$w_a(L/2)$	$u_a(L,h)$	$\sigma_a(L/2,h)$	$\tau_a(0,0)$
Pagano [19] (reference)	-2.8949	0.9391	18.6899	1.4306
ZZ-EXP-RED90 (present)	-2.8970 $\epsilon_{rel} = 0.07\%$	0.9416 $\epsilon_{rel} = 0.27\%$	18.4887 $\epsilon_{rel} = 1.07\%$	1.4132 $\epsilon_{rel} = 1.22\%$
ZZ-EXP-KRU49 (present)	-2.8970 $\epsilon_{rel} = 0.07\%$	0.9416 $\epsilon_{rel} = 0.27\%$	18.4887 $\epsilon_{rel} = 1.07\%$	1.4132 $\epsilon_{rel} = 1.22\%$
ZZ-EXP-TOU91 (present)	-2.8844 $\epsilon_{rel} = 0.36\%$	0.9571 $\epsilon_{rel} = 1.92\%$	18.7927 $\epsilon_{rel} = 0.55\%$	1.4022 $\epsilon_{rel} = 1.99\%$
ZZ-EXP-SOL92 (present)	-2.8978 $\epsilon_{rel} = 0.10\%$	0.9402 $\epsilon_{rel} = 0.12\%$	18.4600 $\epsilon_{rel} = 1.23\%$	1.4142 $\epsilon_{rel} = 1.15\%$
ZZ-EXP-KAR02 (present)	-2.8659 $\epsilon_{rel} = 1.00\%$	0.9709 $\epsilon_{rel} = 3.39\%$	19.0646 $\epsilon_{rel} = 2.00\%$	1.3921 $\epsilon_{rel} = 2.69\%$
ZZ-EXP-AKA07 (present)	-2.8889 $\epsilon_{rel} = 0.21\%$	0.9525 $\epsilon_{rel} = 1.43\%$	18.7016 $\epsilon_{rel} = 0.06\%$	1.4055 $\epsilon_{rel} = 1.75\%$
ZZ-MUR [11]	-2.8033 $\epsilon_{rel} = 3.16\%$	0.8248 $\epsilon_{rel} = 12.17\%$	16.1942 $\epsilon_{rel} = 13.35\%$	1.4359 $\epsilon_{rel} = 0.37\%$
VIDAL [16]	-2.8026 $\epsilon_{rel} = 3.19\%$	0.9929 $\epsilon_{rel} = 5.73\%$	19.4954 $\epsilon_{rel} = 4.31\%$	1.4284 $\epsilon_{rel} = 0.15\%$
LW Lu e Liu [21]	-2.9112 $\epsilon_{rel} = 0.56\%$	0.9396 $\epsilon_{rel} = 0.05\%$	18.4494 $\epsilon_{rel} = 1.27\%$	1.4256 $\epsilon_{rel} = 0.35\%$

The values of w_j , u_{0j} , Φ_j and ψ_j are obtained by replacing Eq. (14) in Eq. (11) and solving the obtained algebraic system.

3. Results and Discussion

The results are dimensionless, according to Eq. (15) [19]. L , b , and $2h$ are the length, width and thickness of the cross section, respectively. E_α and $G_{\alpha\beta}$ ($\alpha, \beta \in \{x, y, z\}$) are the longitudinal and transverse moduli of elasticity, respectively. To obtain the shear stress field, this study uses the equilibrium equation, as presented in [20]:

$$\begin{aligned}
 u_a^{(k)}(x,z) &= u^{(k)}(x,z) \frac{bE_y}{2hq_0}, \quad w_a(x) = w(x) \frac{800bh^3E_y}{L^4q_0}, \quad S = \frac{L}{2h}, \\
 \sigma_a^{(k)}(x,z) &= \sigma^{(k)}(x,z) \frac{b}{q_0}, \quad \tau_a^{(k)}(x,z) = \tau^{(k)}(x,z) \frac{b}{q_0}, \quad \bar{x} = S \frac{x}{L}, \quad \bar{z} = \frac{z}{(2h)},
 \end{aligned}
 \tag{15}$$

where $\bar{x} \in [0, S]$ and $\bar{z} \in [-1/2, 1/2]$.

For the fiber-reinforced laminated beams, the following elastic properties (graphite/epoxy composite [19]) were used in the examined instances:

$$E_x = 25MPa \quad E_y = 1MPa \quad G_{xy} = 0.5MPa \quad G_{yz} = 0.2MPa \quad \nu_{xy} = \nu_{yz} = 0.25$$

The accuracy of high-order beam theories (RED90, KRU49, SOL92, KAR03, and AKA07) combined with the exponential zigzag function in obtaining the response fields proposed in this work was tested, and the nomenclature used to identify these combinations of theories was made by composing ZZ-EXP-(beam theory); for example, ZZ-EXP-RED90 indicates the Reddy function [4] (see Table 1), and the exponential ZZ function (Eq. (4)) is used in the proposed unified kinematics (Eq. (1)) as $f(z)$ and $\Phi_{zz}^{(k)}(z)$, respectively. Once this procedure is completed, the sequence of the other equations remains valid for any beam theory presented in Table 1. Additionally, the linear zigzag function of Murakami [11] and the zigzag function presented by VIDAL [16] were analyzed. For reference, the results obtained using the LW theory [21] and the theory of elasticity developed by Pagano [19] were adopted for cross-ply laminated beams.

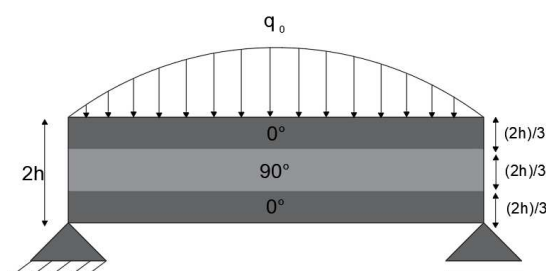


Fig. 4. Geometric, loading, and boundary conditions.



Table 3. W.A.P.E. metric calculated for Example 1.

Model	$w_a(x)$	$u_a(L, z)$	$\sigma_a(L / 2, z)$	$\tau_a(0, z)$
ZZ-EXP-RED90 (present)	0.17%	6.20%	3.79%	1.28%
ZZ-EXP-KRU49 (present)	0.17%	6.20%	3.79%	1.28%
ZZ-EXP-TOU91 (present)	0.86%	7.95%	4.49%	1.73%
ZZ-EXP-SOL92 (present)	0.24%	6.05%	3.79%	1.23%
ZZ-EXP-KAR02 (present)	2.38%	9.75%	6.34%	2.17%
ZZ-EXP-AKA07(present)	0.50%	7.36%	4.07%	1.60%
LW [21]	1.34%	4.00%	2.72%	1.70%
ZZ-MUR [11]	7.52%	15.51%	12.77%	1.91%
VIDAL [16]	7.58%	11.96%	10.71%	1.33%

3.1 Example 1

As shown in Fig. 4, this example refers to a simply supported beam with a cross-section ($b \times 2h$) and length L formed by three laminae with fibers oriented at $[0^\circ/90^\circ/0^\circ]^T$. The layers had equal thicknesses and $S = 4$ (moderately thick beams). The structure was subjected to sinusoidal distributed loading, represented by $q(x) = \sum_{j=1}^{\infty} q_j \sin(j\pi x / L)$ with $q_j = q_0$ ($j = 1$).

The first analysis compared the maximum values of the axial and transverse displacements and normal and shear stresses. Table 2 presents the reference values of Pagano [19] and the LW theory proposed by Lu and Liu [21]. Table 2 lists the relative errors obtained using ZZ-EXP (combined with several beam theories), ZZ-MUR [11], and VIDAL [16] for several dimensionless response fields (Eq. (15)).

Table 2 shows that minor relative errors in the maximum transverse displacement values were obtained for the ZZ-EXP-RED90, ZZ-EXP-KRU49, and ZZ-EXP-SOL92 combinations. From the analysis of the axial displacement, the combination of ZZ-EXP-SOL92 presented the best results. Regarding the study of the maximum normal stress, the highlight is the combination of the AKA07 function. Finally, for the shear stress, the best combination was observed for the SOL92 function. As shown in Table 2, ZZ-EXP-RED90, ZZ-EXP-KRU49, ZZ-EXP-SOL92, and ZZ-EXP-AKA07 exhibited the lowest relative errors, highlighting ZZ-EXP-SOL92 for the regularity of their results among the ZZ-EXP functions.

In the comparison between the ZZ-EXP functions and the proposals of [11], [16], and [21], Table 2 shows that the MUR-ZZ model [11] presents higher relative errors in almost all analyses compared to all combinations of the ZZ-EXP function, highlighting the importance of using higher-order functions. The ZZ-MUR model showed a minor relative error in the shear stress; however, this was because the response field was determined using equilibrium equations. If directly calculated using the Murakami function [11], the results would show very high values of relative error. By increasing the order of the zigzag function from the linear model by Murakami [11] to the high-order model by Vidal [16], it can be observed in Table 2 that ZZ-EXP-SOL92, ZZ-EXP-RED90, and ZZ-EXP-KRU49 continue to perform better. Finally, the ZZ-EXP-SOL92 function presented relative errors close to those obtained by the LW theory [21], with the model in [21] having the inconvenience of the number of unknowns being proportional to the number of layers.

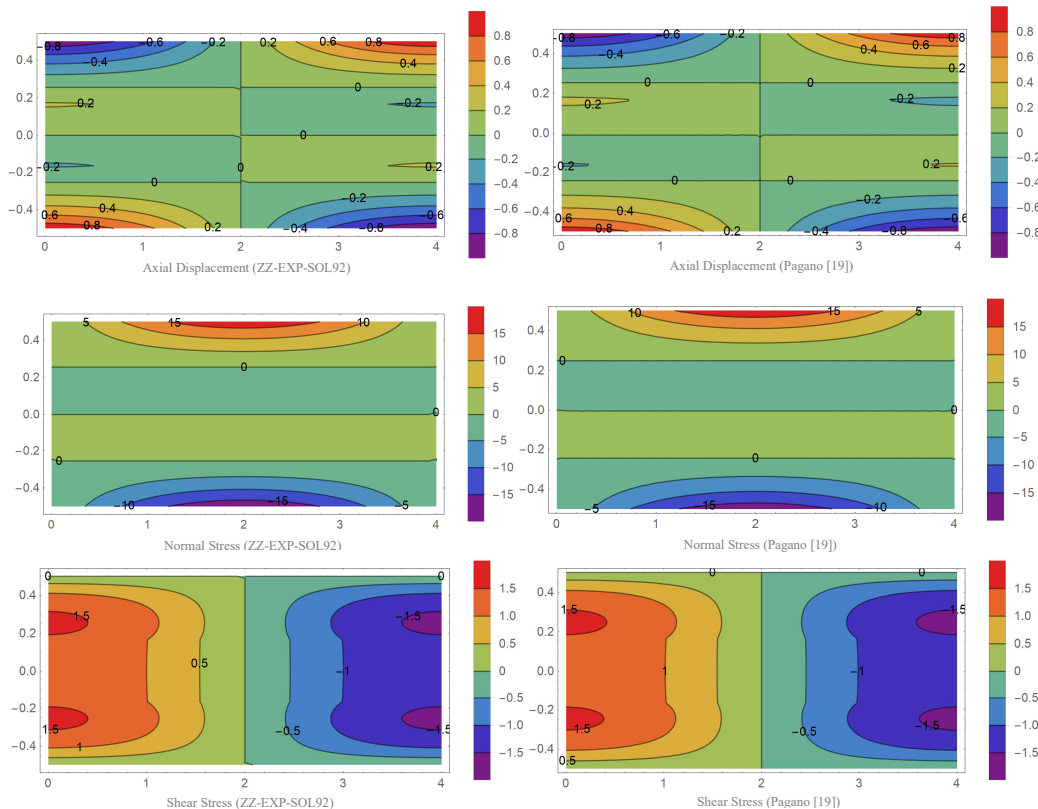


Fig. 5. Variations of the displacements and stress within a laminated beam dimensionless $\bar{x} \times \bar{z}$ for Example 1.



Table 4. Maximum values and errors relative to Example 2.

$f(z)$	$w_a(L/2)$	$u_a(L,h)$	$\sigma_a(L/2,h)$	$\tau_a(0,0)$
Pagano [19] (reference)	-3.8145	1.1637	23.0636	1.7616
ZZ-EXP-SOL92 (present)	-3.7935	1.1673	22.9202	1.7962
	$\epsilon_{rel} = 0.55\%$	$\epsilon_{rel} = 0.30\%$	$\epsilon_{rel} = 0.62\%$	$\epsilon_{rel} = 1.96\%$
ZZ-MUR [11]	-3.1172	0.9711	32.2647	1.8251
	$\epsilon_{rel} = 18.28\%$	$\epsilon_{rel} = 16.55\%$	$\epsilon_{rel} = 39.89\%$	$\epsilon_{rel} = 3.60\%$
VIDAL [16]	-3.4211	1.3233	26.5724	1.5819
	$\epsilon_{rel} = 11.12\%$	$\epsilon_{rel} = 15.26\%$	$\epsilon_{rel} = 13.43\%$	$\epsilon_{rel} = 9.61\%$

Table 5. W.A.P.E. metric Calculated for Example 2.

$f(z)$	$w_a(x)$	$u_a(L,z)$	$\sigma_a(L/2,z)$	$\tau_a(0,z)$
ZZ-EXP-SOL92	1.44%	10.06%	7.23%	2.54%
ZZ-MUR [11]	19.01%	35.63%	68.15%	4.54%
VIDAL [16]	11.12%	27.77%	23.68%	11.73%

Next, the error analysis for a given section was no longer limited to the maximum values. As a parameter to quantify discrepancies between calculated and reference values in [19], the statistical metric "weighted absolute percentage error" (W.A.P.E.) presented in Eq. (16) is used, where x_j are the calculated values and X_j are the reference values. The values calculated for $w_a(x)$, $u_a(L,z)$, $\sigma_a(L/2,z)$ and $\tau_a(0,z)$ using the W.A.P.E. metric are listed in Table 3.

$$W.A.P.E.(%) = 100 \frac{\sum_{j=1}^n |x_j - X_j|}{\sum_{j=1}^n |X_j|} \tag{16}$$

Table 3 shows that all ZZ-EXP combinations present minor error values calculated using the W.A.P.E. metric compared to ZZ-MUR [11] and Vidal [16]. However, the ZZ-EXP model exhibits a performance similar to that of the LW model [21]. In this comparison, the ZZ-EXP model showed better results for $w_a(x)$ and $\tau_a(0,z)$, whereas the LW [21] performed better for $u_a(L,z)$ and $\sigma_a(L/2,z)$. Notably, the ZZ-EXP model does not increase the number of unknowns as the number of layers increases, as shown by the LW model [21].

From 4,743 coordinates uniformly spread throughout the laminated composite beam, the response fields were calculated using the ZZ-EXP-SOL92 model and the reference in [19]. In Fig. 5, excellent agreement between the proposed and reference models is observed, qualitatively evidenced by the similarity in the color gradient distribution between the compared models.

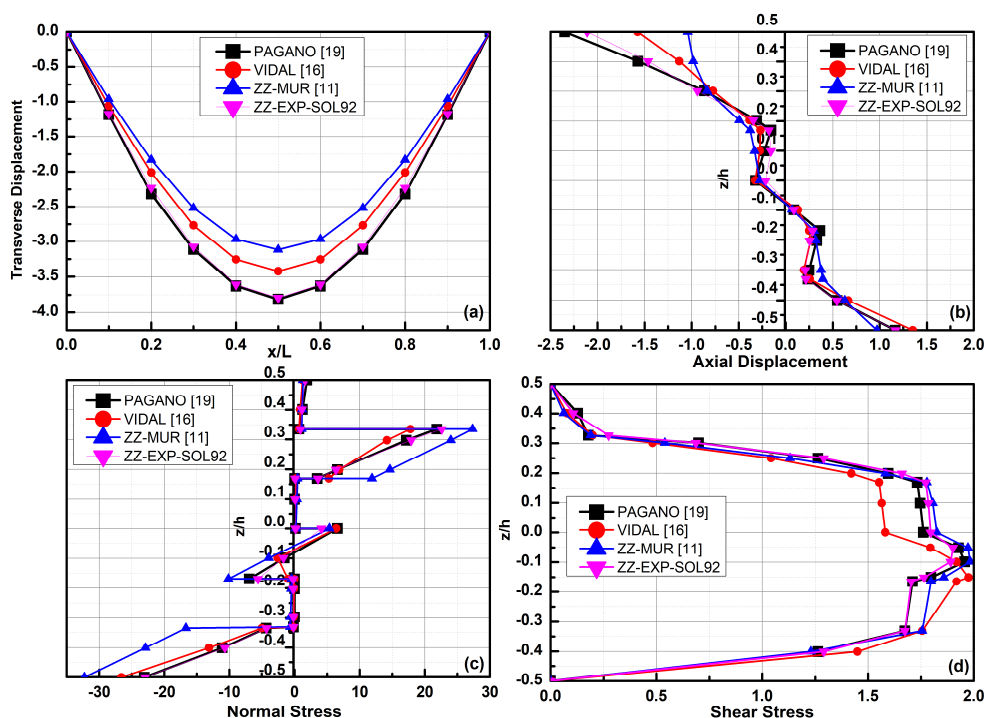


Fig. 6. Variation of response fields in Example 2 for (a) $w_a(x)$, (b) $u_a(L,z)$, (c) $\sigma_a(L/2,z)$, and (d) $\tau_a(0,z)$, where $z \in [-h/2, h/2]$.



3.2 Example 2

In this example, a simply supported beam comprising six layers with fibers oriented at $[0^\circ/90^\circ]_3$ (asymmetric stacking) was analyzed. The laminate was considered regular, adopting the parameter $S = 4$ for loading, similar to that in Example 1.

In this analysis, the results of Pagano [19] were compared with those of the linear function ZZ-MUR [11], higher-order function VIDAL [16], and exponential function ZZ-EXP-SOL92 because the latter presented better results among the combinations of the ZZ-EXP function shown in Example 1. The maximum values (Table 4) and W.A.P.E. metric (Table 5) for transverse displacement along the longitudinal axis, axial displacement ($x = L$), normal stress ($x = L/2$), and shear stress ($x = 0$) were calculated for the cross-sections. The qualitative behaviors of ZZ-MUR [11], Vidal [16], ZZ-EXP-SOL92, and Pagano [19] for $w_a(x)$, $u_a(L,z)$, $\sigma_a(L/2,z)$ and $\tau_a(0,z)$ are shown in Fig. 6.

Tables 4 and 5 show that the ZZ-EXP-SOL92 model has a minor relative error compared with the ZZ-MUR [11] and Vidal [16] models. This analysis considers the maximum or several values for a given cross-section or along its longitudinal axis (W.A.P.E. metric). Compared to the results of Example 1 with three layers, in this case with six layers, a loss of accuracy in the models proposed in [11] and [16] was observed when compared with the reference model in [19]. However, the model ZZ-EXP-SOL92, here presented, proved to be stable with respect to accuracy when the number of layers increased. Qualitatively, Fig. 6 shows the agreement between the proposed model ZZ-EXP-SOL92 (lines in pink lines) and the reference model proposed by Pagano [19] (black line). Simultaneously, the Vidal [16] and ZZ-MUR [11] models presented discrepancies in all the response fields analyzed, with more significant distortions for the transverse displacement and shear stress compared to the reference.

From the 9,486 coordinates uniformly spread throughout the laminated composite beam, the response fields were calculated using the ZZ-EXP-SOL92 model and the reference in [19]. In Fig. 7, excellent agreement between the proposed and reference models is observed, which is qualitatively evidenced by the similarity in the color gradient distribution between the compared models.

3.3 Example 3

In this example, a beam is analyzed with the same geometric conditions, loading, and parameter $S = 4$ as in the previous analysis; however, it consists of 11 regular layers reinforced by fibers with the following stacking sequence: $[0^\circ/90^\circ/0^\circ/90^\circ/0^\circ/90^\circ]_6$. Tables 6 and 7 list the maximum values and W.A.P.E. metrics, respectively. Based on the results reported by Pagano [11], the relative errors listed in Tables 6 and 7 were calculated for ZZ-EXP-SOL92 (proposed), ZZ-MUR [11], and Vidal [16]. In Fig. 8, the qualitative results are presented for the (a) transverse displacement along the longitudinal axis, (b) axial displacement for the cross-section at $x = L$, (c) normal stress for the cross-section at $x = L/2$, and (d) shear stress for the cross section $x = 0$.

In Tables 6 and 7, a small distance between the values of the ZZ-EXP-SOL92 model and the reference values in [19] can be quantitatively observed, whereas Models [11] and [16] present values that differ significantly from the reference values. Fig. 8 qualitatively shows the excellent fit of the proposed model (pink line) to the reference values (black line), which does not always occur when using Models [11] or [16]. According to the results presented in Examples 1, 2, and 3, it is possible to verify that the proposed ZZ-EXP-SOL92 model maintains low errors, regardless of the number of layers. In the ZZ-MUR [11] and Vidal [16] models, the errors increased with the number of layers.

From the 17,391 coordinates uniformly spread throughout the laminated composite beam, the response fields were calculated using the ZZ-EXP-SOL92 model and the reference in [19]. In Fig. 9, excellent agreement between the proposed and reference models is observed, qualitatively evidenced by the similarity in the color gradient distribution between the compared models.

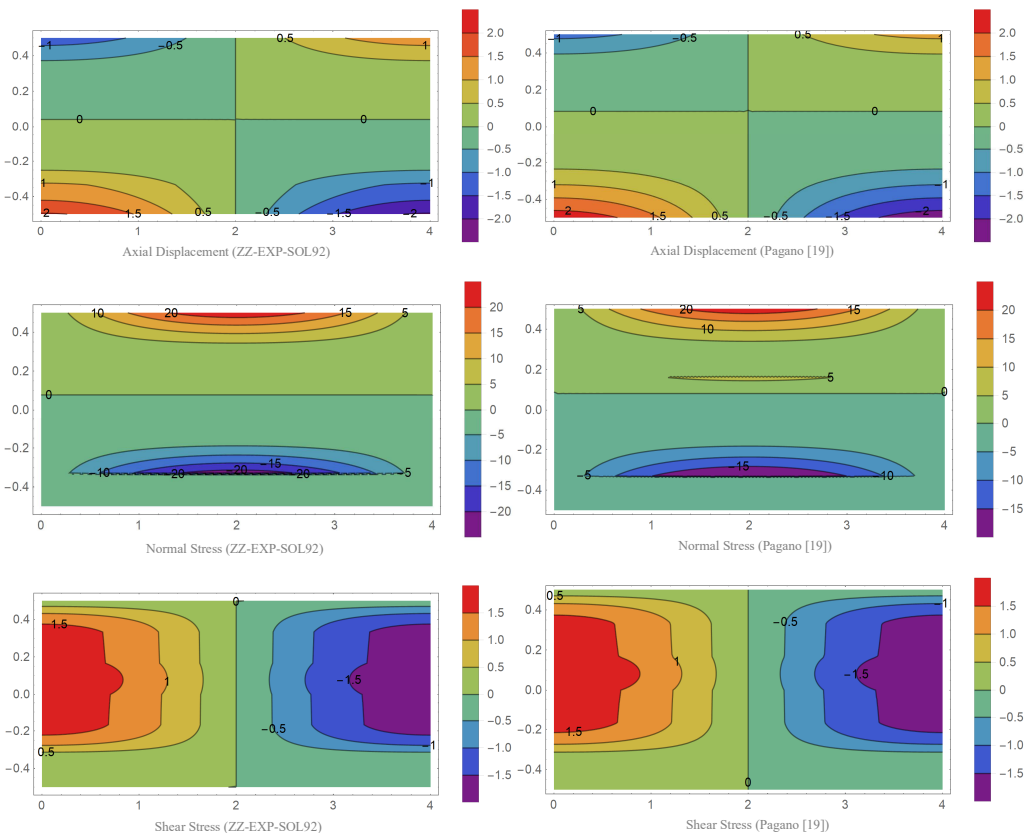


Fig. 7. Variations of the displacement and stress within a laminated beam dimensionless $\bar{x} \times \bar{z}$ for Example 2.



Table 6. Maximum values and relative errors for Example 3.

$f(z)$	$w_a(L/2)$	$u_a(L,h)$	$\sigma_a(L/2,h)$	$\tau_a(0,0)$
Pagano [19] (reference)	-3.2184	1.0209	20.4828	1.6248
ZZ-EXP-SOL92 (present)	-3.2071	1.0338	20.2980	1.6338
	$\epsilon_{rel} = 0.35\%$	$\epsilon_{rel} = 1.26\%$	$\epsilon_{rel} = 0.90\%$	$\epsilon_{rel} = 0.55\%$
ZZ-MUR [11]	-3.0523	0.8568	16.8233	1.77622
	$\epsilon_{rel} = 5.16\%$	$\epsilon_{rel} = 16.08\%$	$\epsilon_{rel} = 17.87\%$	$\epsilon_{rel} = 9.32\%$
VIDAL [16]	-2.9855	1.1601	22.7777	1.5030
	$\epsilon_{rel} = 7.24\%$	$\epsilon_{rel} = 13.63\%$	$\epsilon_{rel} = 11.20\%$	$\epsilon_{rel} = 7.49\%$

Table 7. W.A.P.E metric for Example 3.

$f(z)$	$w_a(x)$	$u_a(L,z)$	$\sigma_a(L/2,z)$	$\tau_a(0,z)$
ZZ-EXP-SOL92	0.35%	3.11%	5.03%	0.65%
ZZ-MUR [11]	5.16%	22.28%	25.14%	7.30%
VIDAL [16]	7.24%	19.25%	18.04%	5.53%

3.4 Slenderness analysis (S parameter)

In this section, a study is carried out regarding the dependence of the response fields on the slenderness index of the beam, characterized by the parameter S. The analysis of the structure of both thick and thin beams is carried out by varying the parameter S from 4 to 40. In this analysis, the geometric and stacking characteristics of the layers were the same as those used in Example 1. Table 8 presents the maximum values for the transverse displacement fields at $x = L/2$ and axial displacement at $(x = L, z = h)$. Additionally, Table 9 shows the maximum values for normal stress, at $(x, z) = (L/2, h)$, and for shear stress, at $(x, z) = (0, 0)$. Tables 8 and 9 present the results obtained for the different ZZ-EXP models used in this work and compares them with the reference results obtained by the elasticity theory in [19].

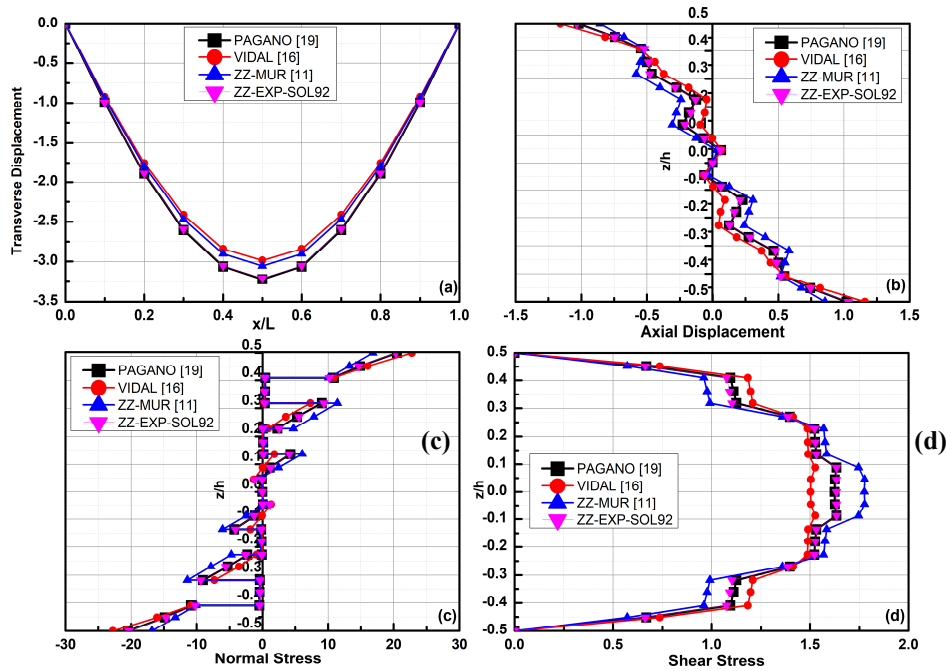


Fig. 8. Variation of response fields in Example 3 for (a) $w_a(x)$, (b) $u_a(L,z)$, (c) $\sigma_a(L/2,z)$, and (d) $\tau_a(0,z)$, where $z \in [-h/2, h/2]$.

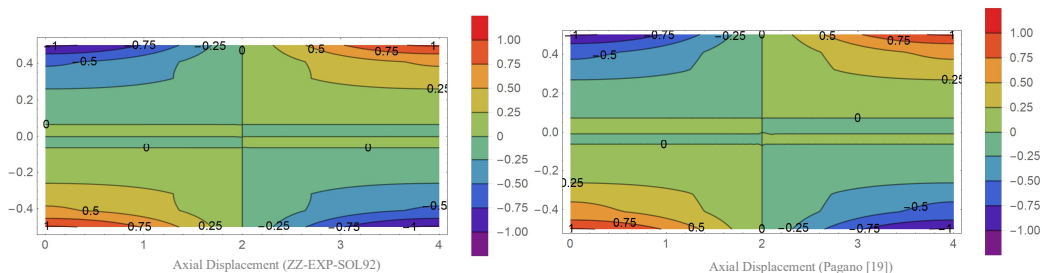


Fig. 9. Variations of the displacements and stress within a laminated beam dimensionless $\bar{x} \times \bar{z}$ for Example 3.



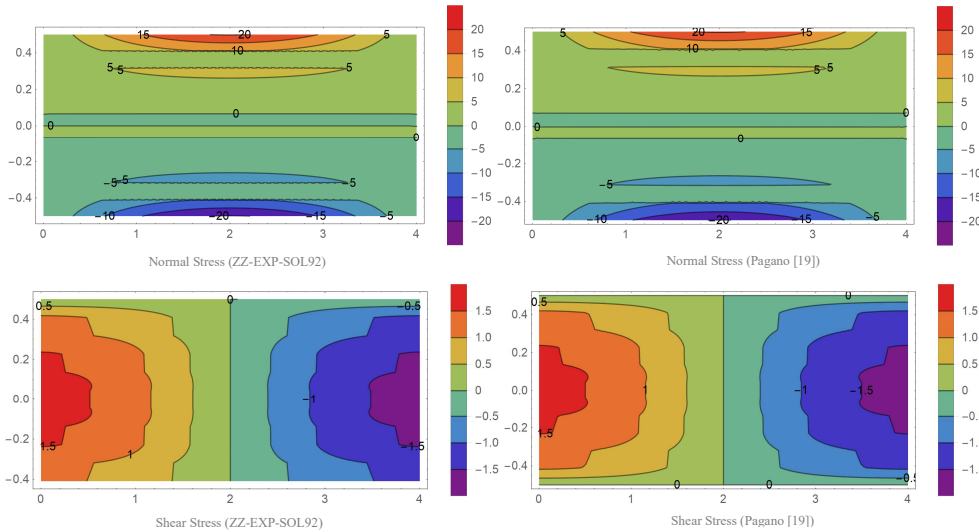


Fig. 9. Continued.

Table 8. Maximum values of the transverse displacement, $w_a(L/2)$ and axial displacement $u_a(L, h)$.

S	Transverse displacement				Axial displacement			
	4	10	20	40	4	10	20	40
PAGANO [19]	-2.8949	-0.9307	-0.6172	-0.5367	0.9391	9.3487	66.7796	518.0090
ZZ-EXP - RED90	-2.8970 $\epsilon_{rel} = 0.07\%$	-0.9323 $\epsilon_{rel} = 0.17\%$	-0.6181 $\epsilon_{rel} = 0.15\%$	-0.5378 $\epsilon_{rel} = 0.20\%$	0.9416 $\epsilon_{rel} = 0.27\%$	9.2491 $\epsilon_{rel} = 1.06\%$	66.7087 $\epsilon_{rel} = 0.11\%$	518.6815 $\epsilon_{rel} = 0.13\%$
ZZ-EXP - KRU49	-2.8970 $\epsilon_{rel} = 0.07\%$	-0.9323 $\epsilon_{rel} = 0.17\%$	-0.6181 $\epsilon_{rel} = 0.15\%$	-0.5378 $\epsilon_{rel} = 0.20\%$	0.9416 $\epsilon_{rel} = 0.27\%$	9.2491 $\epsilon_{rel} = 1.06\%$	66.7087 $\epsilon_{rel} = 0.11\%$	518.6815 $\epsilon_{rel} = 0.13\%$
ZZ-EXP - TOU91	-2.8844 $\epsilon_{rel} = 0.36\%$	-0.9332 $\epsilon_{rel} = 0.27\%$	-0.6184 $\epsilon_{rel} = 0.19\%$	-0.5379 $\epsilon_{rel} = 0.20\%$	0.9571 $\epsilon_{rel} = 1.92\%$	9.3005 $\epsilon_{rel} = 0.52\%$	66.8164 $\epsilon_{rel} = 0.05\%$	518.8995 $\epsilon_{rel} = 0.17\%$
ZZ-EXP - SOL92	-2.8978 $\epsilon_{rel} = 0.10\%$	-0.9322 $\epsilon_{rel} = 0.16\%$	-0.6180 $\epsilon_{rel} = 0.13\%$	-0.5378 $\epsilon_{rel} = 0.20\%$	0.9402 $\epsilon_{rel} = 0.12\%$	9.2444 $\epsilon_{rel} = 1.11\%$	66.6987 $\epsilon_{rel} = 0.12\%$	518.6613 $\epsilon_{rel} = 0.13\%$
ZZ-EXP - KAR03	-2.8659 $\epsilon_{rel} = 1.00\%$	-0.9330 $\epsilon_{rel} = 0.25\%$	-0.6185 $\epsilon_{rel} = 0.21\%$	-0.5379 $\epsilon_{rel} = 0.22\%$	0.9709 $\epsilon_{rel} = 3.39\%$	9.3481 $\epsilon_{rel} = 0.06\%$	66.9166 $\epsilon_{rel} = 0.21\%$	519.1026 $\epsilon_{rel} = 0.21\%$
ZZ-EXP - AKA07	-2.8889 $\epsilon_{rel} = 0.21\%$	-0.9330 $\epsilon_{rel} = 0.25\%$	-0.6184 $\epsilon_{rel} = 0.19\%$	-0.5379 $\epsilon_{rel} = 0.22\%$	0.9525 $\epsilon_{rel} = 1.43\%$	9.2850 $\epsilon_{rel} = 0.68\%$	66.7839 $\epsilon_{rel} = 0.06\%$	518.8336 $\epsilon_{rel} = 0.16\%$

Table 9. Maximum values for normal stress $\sigma_a(L/2, h)$ and shear stress $\tau_a(0, 0)$.

S	Normal stress				Shear stress			
	4	10	20	40	4	10	20	40
PAGANO [19]	18.6899	73.6088	263.1913	1019.6630	1.4306	4.2381	8.7493	17.6447
ZZ-EXP - RED90	18.4887 $\epsilon_{rel} = 1.07\%$	72.6425 $\epsilon_{rel} = 1.31\%$	261.9645 $\epsilon_{rel} = 0.47\%$	1018.4287 $\epsilon_{rel} = 0.12\%$	1.4132 $\epsilon_{rel} = 1.22\%$	4.2466 $\epsilon_{rel} = 0.20\%$	8.7541 $\epsilon_{rel} = 0.05\%$	17.6444 $\epsilon_{rel} = 0.02\%$
ZZ-EXP - KRU49	18.4887 $\epsilon_{rel} = 1.07\%$	72.6425 $\epsilon_{rel} = 1.31\%$	261.9645 $\epsilon_{rel} = 0.47\%$	1018.4287 $\epsilon_{rel} = 0.12\%$	1.4132 $\epsilon_{rel} = 1.22\%$	4.2466 $\epsilon_{rel} = 0.20\%$	8.7541 $\epsilon_{rel} = 0.05\%$	17.6444 $\epsilon_{rel} = 0.02\%$
ZZ-EXP - TOU91	18.7927 $\epsilon_{rel} = 0.55\%$	73.0461 $\epsilon_{rel} = 0.77\%$	262.3875 $\epsilon_{rel} = 0.31\%$	1018.8568 $\epsilon_{rel} = 0.08\%$	1.4022 $\epsilon_{rel} = 1.99\%$	4.2403 $\epsilon_{rel} = 0.05\%$	8.7507 $\epsilon_{rel} = 0.02\%$	17.6427 $\epsilon_{rel} = 0.01\%$
ZZ-EXP - SOL92	18.4600 $\epsilon_{rel} = 1.23\%$	72.6049 $\epsilon_{rel} = 1.36\%$	261.9254 $\epsilon_{rel} = 0.48\%$	1018.3891 $\epsilon_{rel} = 0.12\%$	1.4142 $\epsilon_{rel} = 1.15\%$	4.2471 $\epsilon_{rel} = 0.21\%$	8.7544 $\epsilon_{rel} = 0.06\%$	17.6446 $\epsilon_{rel} = 0.01\%$
ZZ-EXP - KAR03	19.0646 $\epsilon_{rel} = 2.00\%$	73.4197 $\epsilon_{rel} = 0.26\%$	262.7811 $\epsilon_{rel} = 0.16\%$	1019.2557 $\epsilon_{rel} = 0.04\%$	1.3921 $\epsilon_{rel} = 2.69\%$	4.2342 $\epsilon_{rel} = 0.09\%$	8.7475 $\epsilon_{rel} = 0.02\%$	17.6411 $\epsilon_{rel} = 0.02\%$
ZZ-EXP - AKA07	18.7016 $\epsilon_{rel} = 0.06\%$	72.9242 $\epsilon_{rel} = 0.93\%$	262.2596 $\epsilon_{rel} = 0.35\%$	1018.7274 $\epsilon_{rel} = 0.09\%$	1.4055 $\epsilon_{rel} = 1.75\%$	4.2421 $\epsilon_{rel} = 0.09\%$	8.7517 $\epsilon_{rel} = 0.03\%$	17.6433 $\epsilon_{rel} = 0.02\%$



From Tables 8 and 9, it can be observed that the relative errors remain stable regardless of the variation of the parameter S . For slender beams ($S = 40$), the relative errors obtained by each ZZ-EXP model are identical, with only slight differences when the beam thickens ($S = 4$). Additionally, the models ZZ-EXP-SOL92, ZZ-EXP-RED90, and ZZ-EXP-KRU49 present similar accuracy with a slight improvement compared to the other models.

4. Conclusion

This study proposed a new zigzag function, referred to as ZZ-EXP, and its accuracy was compared with other existing functions in the literature, such as Murakami's zigzag function (ZZ-MUR) [11] and the function presented by Vidal [16]. In addition, this study compared the zigzag theory by incorporating the proposed model with the LW theory [21] and, as a reference, the results of the elasticity theory developed by Pagano [19]. The analysis was conducted for three examples of stacks of a simply supported laminated beam. In Examples 1, 2 and 3, the fiber orientations were adopted as $[0^\circ/90^\circ/0^\circ]^T$, $[0^\circ/90^\circ]_b$ and $[0^\circ/90^\circ/0^\circ/90^\circ/0^\circ/90^\circ]_s$, respectively. The final analysis evaluated the dependence of the maximum values of the response fields on the S -parameter. From the results presented, the combination of kinematics with zigzag functions, which are both of high order, provided significant improvements in accuracy, which was confirmed by the comparison between the ZZ-EXP models (high order) and the ZZ-MUR function [11] (low order). The proposed model (ZZ-EXP) was compared with Vidal's improved model [16], and the ZZ-EXP results showed lower relative errors, as listed in Tables 2–7. The proposed model was also stable in controlling the relative error, with minor values, as the number of laminate layers increased, which was not observed for Models [11, 16], making the proposed model (ZZ-EXP) attractive for many other applications. As established in the literature, the LW approach usually presents greater accuracy than ZZ theories. However, the present proposal proved to be compatible with the LW theory in terms of precision and convenience of not increasing the number of unknowns as the number of layers increases, which is absent in LW. Subsequently, the ZZ-EXP function, in combination with other higher-order kinematics of the beams, was not influenced by variations in the S parameter. Given the combination of the ZZ-EXP function with high-order kinematics, ZZ-EXP-RED90, ZZ-EXP-KRU49, and ZZ-EXP-SOL92 generally exhibit lower relative errors when referenced in [19].

Author Contributions

L.F. Prado Leite developed the mathematical modeling and proposed functions, and F.C. Da Rocha initiated the project and analyzed the results. The manuscript was written with contributions from all authors. All authors discussed the results, reviewed and approved the final version of the manuscript.

Acknowledgments

The authors thank the Postgraduate Program in Civil Engineering at the Federal University of Sergipe (PROEC/UFS) for providing the necessary infrastructure for developing this study.

Conflict of Interest

The authors declare no conflicts of interest concerning the research, authorship, or publication of this article.

Funding

This work was financially supported by the CNPq (Process No. 402857/2021-6) and a research grant from CAPES.

Data Availability Statements

The datasets generated and/or analyzed in the current study are available from the corresponding author upon reasonable request.

Nomenclature

L	Beam length	$\Psi(x)$	Amplitude zig-zag function
$q(x)$	Load function on x axis	RED90	Reddy (1990) beam theory
b	Beam width	KRU49	Kruszewski (1949) beam theory
$2h$	Beam height	TOU91	Tourratier (1991) beam theory
$u(x,z)$	Axial displacement	SOL92	Soldatos (1992) beam theory
$w(x)$	Deflection function	KAR03	Karama (2003) beam theory
$f(z)$	High order shear function	AKA07	Akavci (2007) beam theory
$\Phi(x)$	Shear angle	ZZ-MUR	Murakami (1981) zig-zag function
$\Phi_{zz}(z)$	Zigzag function	ZZ-EXP	Exponential zig-zag function
		LW-LL	Layerwise (Liu e Lee, 1990) theory


References


- [1] Sayyad, A.S., Comparison of various refined beam theories for the bending and free vibration analysis of thick beams, *Applied and Computational Mechanics*, 5, 2011, 217-230.
- [2] Timoshenko, S.P., On the correction factor for shear of the differential equation for transverse vibrations of bars of uniform cross-section, *The London Edinburgh, Dublin Philosophical Magazine, and Journal of Science Edinburgh*, 43, 1921, 125-131.
- [3] Kruszewski, E.T., *Effect of transverse shear and rotary inertia on the natural frequency of a uniform beam*, National Advisory Committee for Aeronautics, 1949.
- [4] Reddy, J.N., A general non-linear third order theory of plates with moderate thickness, *International Journal of Nonlinear Mechanics*, 25, 1990, 677-686.
- [5] Tourratier, M., An efficient standard plate theory, *International Journal of Engineering Science*, 1, 1991, 901-916.
- [6] Soldatos, K.P., A transverse shear deformation theory for homogeneous monoclinic plates, *Acta Mechanica*, 94, 1992, 195-220.



- [7] Karama, M., Afaq, K.S., Mistou, S., Mechanical behavior of laminated composite beam by the new multi-layered laminated composite structures model with transverse shear stress continuity, *International Journal of Solids and Structures*, 40, 2003, 1525–1546.
- [8] Akavci, S.S., Buckling and Free Vibration Analysis of Symmetric and Antisymmetric Laminated Composite Plates on an Elastic Foundation, *Journal of Reinforced Plastics and Composites* 26, 2007, 1907–1919.
- [9] Vinson, J.R., Sierakowski, R.L., *The Behavior of Structures Composed of Composite Materials*, Second Ed. Ontario et al., 2008.
- [10] Sayyad, A.S., Ghugal, Y.M., Bending, buckling and free vibration of laminated composite and sandwich beams: A critical review of literature, *Composite Structures*, 171, 2017, 486–504.
- [11] Murakami, H., Maewal, A., Hegemier, G.A., A Mixture Theory with a Director for Linear Elastodynamics of Periodically Laminated Media, *International Journal of Solids and Structures*, 17, 1981, 155–173.
- [12] DI Sciuva, M., A Refined Transverse Shear Deformation Theory for Multilayered Anisotropic Plates, *Atti Accademia delle Scienze di Torino*, 118, 1984, 279–295.
- [13] DI Sciuva, M., An Improved Shear-Deformation Theory for Moderately Thick Multilayered Anisotropic Shells and Plates, *Journal of Applied Mechanics*, 54, 1987, 589–596.
- [14] Tessler, A., DI Sciuva, M., Gherlone, M., A refined zigzag beam theory for composite and sandwich beams, *Journal of Composite Materials*, 43, 2009, 1051–1081.
- [15] Lularon, L., Gherlone, M., Tessler, A., DI Sciuva, M., Assessment of the Refined Zigzag Theory for bending, vibration, and buckling of sandwich plates: a comparative study of different theories, *Composite Structures*, 106, 2013, 777–792.
- [16] Vidal, P., Polit, O., A sine finite element using a zig-zag function for the analysis of laminated composite beams, *Composites Part B: Engineering*, 42, 2011, 1671–1682.
- [17] Zhen, W., Yang, C., Zhang, H. and Zheng, X., Stability of laminated composite and sandwich beams by a Reddy-type higher-order zig-zag theory, *Mechanics of Advanced Materials and Structures*, 26(19), 2019, 1622–1635.
- [18] Prado Leite, L.F., da Rocha, F.C., A novel Higher-Order Zigzag Function Applied to Refined Unified Beam Theory for the Analysis of Composite Laminated Materials, *Periodica Polytechnica Civil Engineering*, 67(3), 2023, 867–874.
- [19] Pagano, N.J., Exact solution for composite laminates in cylindrical bending, *Journal of Composite Materials*, 3, 1969, 398–411.
- [20] Reddy, J.N., *Mechanics of laminated composite plates and shells: Theory and analysis*, Second Edition, Boca Raton, CRC Press, 2004.
- [21] Liu, D., Lu, X., An Interlaminar shear stress continuity theory for laminated composite analysis, *Computers and Structures*, 42, 1992, 9–78.

ORCID iD

L.F. Prado Leite  <https://orcid.org/0000-0002-1854-1425>

F.C. Da Rocha  <https://orcid.org/0000-0002-1054-3397>



© 2023 Shahid Chamran University of Ahvaz, Ahvaz, Iran. This article is an open access article distributed under the terms and conditions of the Creative Commons Attribution-NonCommercial 4.0 International (CC BY-NC 4.0 license) (<http://creativecommons.org/licenses/by-nc/4.0/>).

How to cite this article: Prado Leite L.F., Da Rocha F.C. A Novel Exponential Zigzag Function Coupled High-order Beam Theory for Advanced Laminated Composite Analysis, *J. Appl. Comput. Mech.*, 10(2), 2024, 330–341. <https://doi.org/10.22055/jacm.2023.44907.4286>

Publisher's Note Shahid Chamran University of Ahvaz remains neutral with regard to jurisdictional claims in published maps and institutional affiliations.

